

A short review on joint weak and strong cluster lens-mass reconstruction

Ben D. Normann¹, Kenny Solevåg-Hoti², and Hans Georg Schaathun¹

¹ Department of ICT and Natural Sciences, Norwegian University of Science and Technology, Larsgårdsvegen 2, 6009 Ålesund
e-mail: ben.d.normann@ntnu.no

² The University Library, Norwegian University of Science and Technology, Larsgårdsvegen 2, 6009 Ålesund

Received after we've sent it; accepted at some event E on our future light-cone

ABSTRACT

The divide between weak and strong lensing is of course artificial, in that both regimes are manifestations of the same physical phenomenon: gravity bending the path of light. Nevertheless, these two regimes have to a large extent been treated separately, with different methods. This review traces the development of methods combining weak-lensing and strong-lensing data for joint lens-mass reconstruction, with a particular emphasis on cluster lenses, where both effects occur. We conclude that so-called inverse methods have been successful in merging the two regimes insofar data analysis is concerned. However, a number of improvements seem to be needed. First, not many studies include weak lensing data beyond shear. In light of the unprecedented quality of the data of JWST and future surveys, this is a clear point of improvement. Especially so, since flexion terms have proven useful in determining sub-structures. Second, considering the amount of data available, and the complexity of non-parametric lenses, automating the processes of lens-mass reconstruction would be beneficial. Towards this end, invoking machine learning seems like a promising way forward. The silence of the literature on this latter point is in fact somewhat surprising.

Key words. Cosmology – gravitational lensing – cluster lensing – weak lensing – strong lensing – roulette formalism – roulette expansion – flexion – beyond shear

1. Introduction

The idea of light being bent by gravity, goes back at least to [Newton \(1804\)](#) himself, and later [Mitchell \(1784\)](#) and [Laplace \(1795\)](#). But it was not until the 20th century that it was actually put to use as an observational probe on the universe. Under a solar eclipse in 1905, Eddington and others showed that Einstein's theory of gravity predicted the correct lensing of light, whereas Newton's theory gets it wrong (misses a factor 2). Today, well over a century later, gravitational lensing is recognised as an important cosmological probe, and a rich source of information. One of its uses is the mapping of the (mostly dark) matter in the universe. Mapping the dark matter through gravitational lensing, invokes (cluster) lens-mass reconstruction, which will be the focus of this review.

The effect of gravitational lensing is typically divided into two regimes; weak and strong, both of which are important in understanding complicated lensing structures, such as cluster lenses. Since they are both observational aspects of the same phenomenon, it is natural to wonder to what extent they are still treated separately. This paper reviews the literature on different approaches to merging the two regimes into one unified framework for cluster¹ lens-mass reconstruction.

We take a hybrid approach, combining a structured literature search with a historical approach using prior knowledge and snowball searches. On the one side, we use stringent search criteria, winding up with a total of 29 papers

that we examine in some detail. On the other side, we use previous knowledge and snow-ball searches to complement the historical development. The result is a quasi-historical development.

The rest of the paper is structured as follows. In [Section 2](#) we describe our literature search strategy and study selection. In [Section 3](#), we go on to describe lensing theory in general, before we focus in on the development of (cluster) lens-mass reconstruction in [Section 4](#). This is where the bulk of papers included in the systematic literature review are presented, describing the development up until the state-of-the-art. Finally, in [Section 5](#) we present our concluding remarks.

2. Combining weak and strong: Search method

This review considers the joint use of weak- and strong lensing data for lens-mass reconstruction. To this end a structured search was conducted, as described in this section.

2.1. Search strategy

To create a search string that would effectively capture results relevant to this review we went through several iterations. Searches were made in the Web of Science database, chosen for its breadth and reliability. Attention was restricted to *title*, *abstract* and *keywords*, as it was found unlikely that the relevant literature would omit our search

¹ We focus here on cluster lenses, where both effects occur.

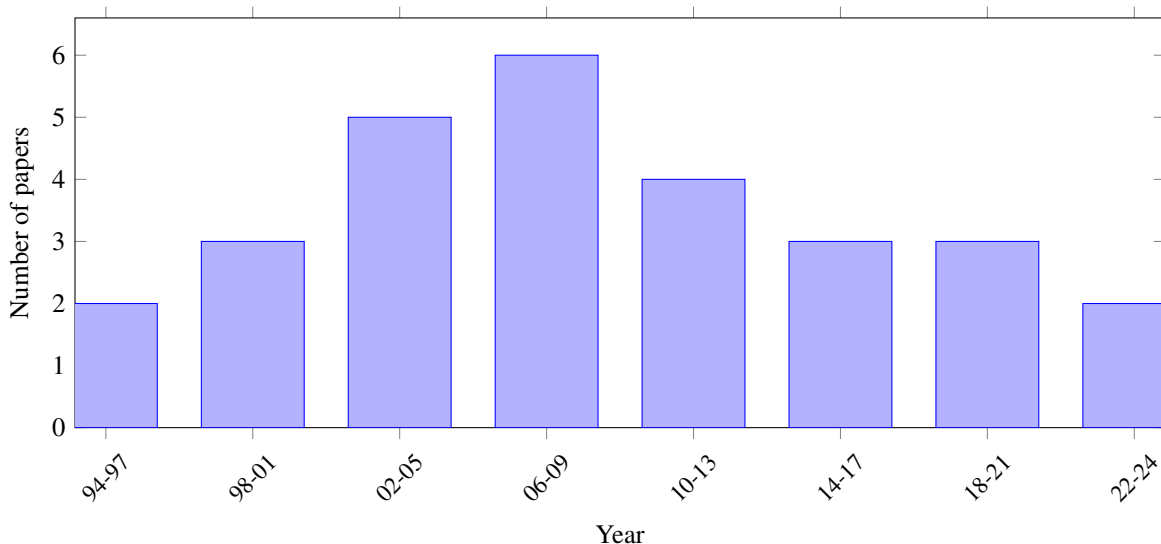


Fig. 1: The histogram shows the number of papers from the shortlist appearing each year, starting in 1994, and with a bin-size of 4 years, except the last bin, which spans 3 years.

Table 1: Preliminary searches in the topic field of the Web of Science database 28th of October 2022

Search	String	Hits
1	weak AND strong AND lens*	1471
2	weak AND strong AND lens* AND reconstruct*	171
3	(combin* OR unit*) AND weak AND strong AND lens* AND reconstruct*	37
4	(combin* OR unit* OR unify* OR join* OR merg* OR bind* OR link* OR expand* OR extend*) AND weak AND strong AND lens* AND reconstruct*	95

words in all these fields. Starting from a broad search we modified the search string to enforce the right context.

The initial search returned articles from a range of unrelated scientific fields. The next iteration narrowed the hits to our field of interest, but with noise still apparent. The main issue was articles where both weak and strong formalisms were used, but handled independently of each other. Correcting for this we made use of words present in highly relevant publications in our next search. These hits were relevant, yet limited our scope. Hence, we readjusted for the possibility of authors using a range of synonyms. This led us to our final query:

(combin* OR unit* OR unify* OR join* OR merg* OR bind* OR link* OR expand* OR extend*) AND weak AND strong AND lens* AND reconstruct*

This search was then applied to the databases Web of Science, Scopus, Compendex and ArXiv providing comprehensive coverage of the field of physics. This resulted in 111 unique papers, when cross-checking the results of the different database searches. The breakdown is given in Table 2.

Going through the abstracts, we selected those papers that concentrated on the theoretical framework for weak and strong lensing. Papers that (judging from the abstracts) seemed to be mere observational ones, or papers that concentrated on theoretical treatment of other observables, such as X-rays, were thus discarded. This discarding-by-abstract step was as such a step of calculated risk, as it might sometimes be hard to judge the novelty of the theoretical methodology underlying an observational study. Especially so, since a successful theoretical method for observational astrophysics is highly dependent on each individual

Table 2: Number of papers found in each database in the search performed on the 28th of October 2022. There are 111 unique papers.

Database	Search field	Hits
Web of Science	Topic	95
Scopus	Title, abstract, keywords	67
ArXiv	Abstract	55
Compendex	Subject, title, abstract	53

observational situation. Nevertheless, if a methodology is particularly novel, one would expect it to be presented in a theoretical paper on its own. Consequently, and performed with some care, this step was taken in order to narrow down the scope of the material.

2.2. Study selection

As a result a total of 29 papers (two of which appeared after the original search was done) were left for deeper scrutiny. This list contained all the papers that were found in an initiation search², before a structured approach was adopted. The final list of 29 papers is presented in Appendix A. Over the course of the next couple of sections we discuss all the 29 papers from the list, in a quasi-historical manner. Snowball searches greatly expanding the list has also been adopted, so that the total number of papers referenced is about five-fold that of the shortlist (29).

It is noteworthy that a whole strand of papers relevant for the topic at hand was, with a couple of exceptions, left out. These were the direct methods extending the weak lensing regime towards the strong regime, by including higher-order effects, such as flexion. Although we have not performed a systematic literature search to include such papers, they are discussed generally in Section 3.4 and in the context of cluster lenses in Sec. 4.7.

² Actually, the most interesting papers were already found in our initial search!

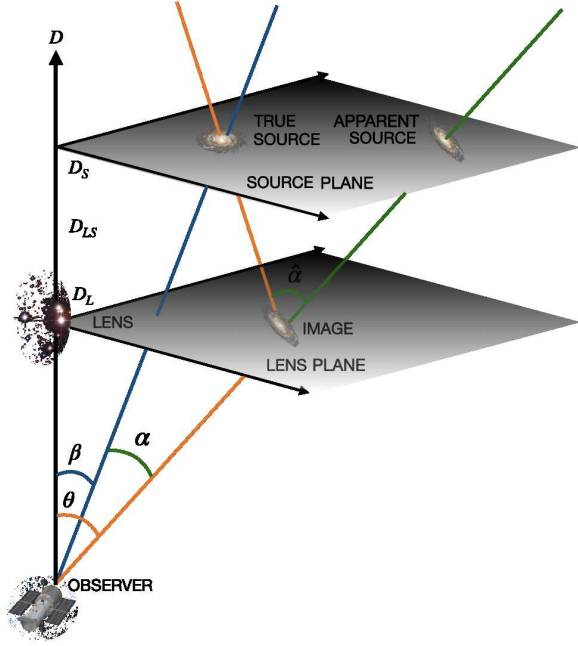


Fig. 2: Lensing geometry. D_L and D_S are angular diameter distances from observer to lens and observer to source, whilst D_{LS} is lens to source. β and θ are angular separations of source and image from the optical axis. The light-ray deflection is denoted by $\hat{\alpha}$, whilst α is the reduced deflection angle.

3. Lensing theory

In the following, we present the basic mathematical framework used in state-of-the-art gravitational lensing. The interested reader is referred to standard texts such as Schneider et al. (1999) (Often denoted SEF) or Schneider et al. (2006) for details, or more recent treatments, like Congdon & C.R. (2018).

The starting point of gravitational lensing is the so-called ray-trace equation

$$\theta D_S = \beta D_S + \hat{\alpha} D_{LS}, \quad (1)$$

which relates angular position θ in the lens plane, at distance D_L from the observer, to corresponding positions β in the source plane, at distance D_S from the observer. This equation follows directly from the geometry assumed in Fig. 2, when equipped with an additional assumption of small angles. The geometry typically³ follows due to a thin-lens approximation, which means that all the mass has been projected down to a two-dimensional plane orthogonal to the optical axis. This is often warranted as the region where the lens affects the light beam is relatively localized, compared to the distances D_L and D_S . In fact, most lens-mass reconstruction techniques seek to reconstruct the 2-dimensional, lens-plane projected mass density. This reveals a fundamental shortcoming of the current capacity of GL. Albeit being standard procedure, the thin-lens approximation cannot reveal three-dimensional structures of a single lens — at least not in a model-free manner. In reality lenses are however three-dimensional, and could be of importance. Take Morandi et al. (2011) as an example, where A1689 is modelled with a triaxial structure. This

³ Not so with the Schwarzschild lens, where exact results are available.

allows to explain discrepancies between x-ray and strong-lensing data as a result of the internal structure of the cluster. As such this demonstrates the importance of taking the 3-dimensional structure of the lens into account in explaining the data.

Defining the reduced deflection angle by

$$\alpha(\theta) \equiv \frac{D_{LS}}{D_S} \hat{\alpha}(\theta), \quad (2)$$

the lens equation is obtained as

$$\beta = \theta - \alpha(\theta). \quad (3)$$

In the thin-lens approximation, one defines the dimensionless surface-mass density κ (also called *convergence*), given by

$$\kappa(\theta) = \frac{\Sigma(\theta)}{\Sigma_{\text{cr}}}. \quad (4)$$

Here Σ is the surface-mass density, and Σ_{cr} is a critical value defined such that

$$\Sigma_{\text{cr}} = \frac{c^2}{4\pi G} \frac{D_s}{D_d D_{ds}}. \quad (5)$$

It is now customary and convenient to define the *lensing potential* ψ (also called the deflection potential) from Poisson's equation for gravity in two dimensions⁴, which takes the form

$$\nabla^2 \psi = 2\kappa. \quad (6)$$

One may use Green's functions to show that an integral solution to this equation is given by

$$\psi(\theta) = \frac{1}{\pi} \int_{\mathbb{R}^2} d^2\theta' \kappa(\theta') \ln|\theta - \theta'|. \quad (7)$$

It follows that the (reduced) deflection angle α may be written as

$$\alpha = \nabla\psi. \quad (8)$$

Using this, the lens equation (3) takes the form

$$\beta = \theta - \nabla\psi(\theta). \quad (9)$$

Consequently, for a given lens ψ , Eq (9) is a mapping $\mathcal{L}_\psi : \mathcal{U} \rightarrow \mathcal{D}$, where \mathcal{U} and \mathcal{D} are sets of undistorted and distorted images, respectively. Since distorted background sources are much smaller than the angular scale on which the lens properties change, the mapping can be locally linearized and the lens mapping (9) may be written as

$$d\beta = \mathcal{A} d\theta \quad (10)$$

where the so-called *amplification matrix* \mathcal{A} is the Jacobian of the coordinate transformation. By way of (9) we have

$$\mathcal{A}(\theta) = \frac{\partial\beta}{\partial\theta} = (\delta_{ij} - \psi_{ij}) \quad \text{where} \quad \psi_{ij} \equiv \frac{\partial^2\psi}{\partial\theta^i\partial\theta^j}. \quad (11)$$

Any Hermitian 2×2 matrix can be decomposed into the identity matrix and the Pauli spin matrices;

$$\mathcal{I} = \begin{pmatrix} 1 & 0 \\ 0 & 1 \end{pmatrix}, \quad \sigma_1 = \begin{pmatrix} 0 & 1 \\ 1 & 0 \end{pmatrix}, \quad (12)$$

$$\sigma_2 = \begin{pmatrix} 0 & -i \\ i & 0 \end{pmatrix}, \quad \sigma_3 = \begin{pmatrix} 1 & 0 \\ 0 & -1 \end{pmatrix}. \quad (13)$$

⁴ The lens plane.

It follows from (9) that \mathcal{A} takes the form

$$\mathcal{A} = (1 - \kappa)\mathcal{I} - \gamma_{\times}\sigma_1 + i\rho\sigma_2 - \gamma_{-}\sigma_3, \quad (14)$$

where standard theory yields $\rho = 0$, since gravity is curl-free at the level of approximation used (refer to Bacon & Schafer (2009) for an interesting discussion). In the above we have defined the (complex) *shear*

$$\gamma = \gamma_+ + i\gamma_{\times} \quad (15)$$

with (real) components

$$\gamma_+ = \frac{1}{2}(\psi_{11} - \psi_{22}), \quad \gamma_{\times} = \psi_{12} = \psi_{21}. \quad (16)$$

By defining the *reduced shear*,

$$g \equiv g_+ + ig_{\times} \quad (17)$$

with components

$$g_+ \equiv \frac{\gamma_+}{1 - \kappa}, \quad g_{\times} \equiv \frac{\gamma_{\times}}{1 - \kappa}, \quad (18)$$

one could alternatively write

$$\mathcal{A} = (1 - \kappa) \begin{pmatrix} 1 - g_+ & -g_{\times} \\ -g_{\times} & 1 + g_+ \end{pmatrix}. \quad (19)$$

From the latter form of \mathcal{A} it is particularly apparent that $(1 - \kappa)$ is a scaling factor, whereas the (reduced) shear alters the shape of the image (by elongation). Consequently, based on the assumption of randomly oriented intrinsic ellipticities in the sources⁵, measurements of image ellipticities yield an estimate of the reduced shear. This may in turn be used to obtain the surface-mass density, as follows. Equation (7), (15) and (16) together give

$$\gamma(\boldsymbol{\theta}) = \frac{1}{\pi} \int_{\mathbb{R}^2} d^2\theta' \mathcal{D}(\boldsymbol{\theta} - \boldsymbol{\theta}') \kappa(\boldsymbol{\theta}'), \quad (20)$$

with

$$\mathcal{D}(\boldsymbol{\theta}) \equiv \frac{\theta_2^2 - \theta_1^2 - 2i\theta_1\theta_2}{|\boldsymbol{\theta}|^4}, \quad (21)$$

That is, γ is a convolution of κ with kernel \mathcal{D} , a relation that may be inverted to give

$$\kappa(\boldsymbol{\theta}) - \kappa_0 = \frac{1}{\pi} \int_{\mathbb{R}^2} d^2\theta' \mathcal{R}e[\mathcal{D}^*(\boldsymbol{\theta} - \boldsymbol{\theta}') \gamma(\boldsymbol{\theta}')]. \quad (22)$$

This relation opens up the possibility of obtaining matter maps of the universe by measuring the shear of distantly incoming light congruences. However, shear in the weak-lensing regime is a relatively weak distortion, and thus relatively hard to detect. In fact, it is necessary to average over large samples of galaxies for the effect to appear. Obtaining the surface-mass density by way of shear measurements have been extensively applied since its first measurement (Tyson et al. 1990). A more modern example is Jauzac et al. (2012). But how is shear actually measured? In the following subsection we provide a more detailed account of the advance of these so-called direct lens-mass reconstructions, based on (22).

⁵ Or otherwise a known distribution of ellipticities.

3.1. Direct lens-mass reconstruction

Obtaining the lens mass via other observables, such as the shear, is known as *lens-mass reconstruction*. The relation (22) was used by Kaiser and Squires (Kaiser & Squires 1993) in developing a parameter-free⁶ inversion technique to obtain the surface-mass density from shear measurements. This inversion technique — hereafter simply referred to as the *KS inversion technique* — quantifies the shear using the quadrupole-moment tensor of the surface brightness (Miralda-Escude 1991); (Miralda-Escude 1991). Following Congdon & C.R. (2018, Chapt. 7), the quadrupole-moment tensor is given by

$$Q_{ij} = \frac{\int_{\mathbb{R}^2} (\theta_i - \bar{\theta}_i)(\theta_j - \bar{\theta}_j) I(\boldsymbol{\theta}) d^2\boldsymbol{\theta}}{\int_{\mathbb{R}^2} I(\boldsymbol{\theta}) d^2\boldsymbol{\theta}}, \quad (23)$$

where $\bar{\boldsymbol{\theta}} = (\bar{\theta}_1, \bar{\theta}_2)$ is the image centroid position, given by

$$\bar{\boldsymbol{\theta}} = \frac{\int_{\mathbb{R}^2} \boldsymbol{\theta} I(\boldsymbol{\theta}) d^2\boldsymbol{\theta}}{\int_{\mathbb{R}^2} I(\boldsymbol{\theta}) d^2\boldsymbol{\theta}}. \quad (24)$$

Note that the KS inversion technique hinges on the assumption that the overall orientation χ of each galaxy is randomly distributed⁷ (ensemble average), so that there is no intrinsic alignment; id est,

$$\langle \chi^2 \rangle = 0. \quad (25)$$

The validity of such an assumption is of course questionable, as reviewed in Troxel & Ishak (2015). Making use of the assumption (25), one may however compare source- and image ellipticities, by such providing a measure of the (reduced) shear. This is in turn inverted to obtain the surface-mass density of the lens. A problem with the method, is that it is valid only for sufficiently weak lensing, where the (complex) distortions δ produced by the lens are linearly related to the shear. In particular one has

$$\delta \approx 2g \approx 2\gamma \quad \text{linear regime} \quad (26)$$

In Schneider & Seitz (1995); Seitz & Schneider (1995), the method is extended to the nonlinear regime, relieving the assumption of weak lensing, as is necessary to probe e.g. the center of clusters. The authors show that in the generalized formulation, the shear is not an observable quantity. The only local observable from image distortions is the (complex) distortion δ , given by

$$\delta = \frac{2g}{1 + |g|^2}, \quad \text{nonlinear regime} \quad (27)$$

with g given in Eq. (17). Evidently, Eq (27) reduces to (26) for $\kappa, \gamma \ll 1$. Another problem with the KS inversion technique is that the inversion formulae is exact only if one assumes observational data on the whole lens plane. The finitude of the CCD or the data field thus causes problems, an issue discussed in various ways in Schneider (1995); Seitz & Schneider (1996); Kaiser et al. (1995); Bartelmann (1995). In the final paper in the series (Seitz & Schneider 1997), redshift information is also taken into account. An improved finite-field inversion method similar to the one

⁶ Or non-parametric. This simply means that no a-priori model for the lens is made, as further discussed in a later section.

⁷ As a side remark: Let it be mentioned that also Tyson et al (1990) assumed that the net alignment of the source galaxies was zero in their detection prior to the work by Kaiser and Squires.

developed in the aforementioned literature is also presented in [Seitz & Schneider \(2001\)](#).

Before the end of the millenium, the KS method had thus been improved to account for

- a. Strong tidal fields (non-linear regime) in cluster centers.
- b. Finite data fields.
- c. Redshift distribution of background galaxies.

The resulting methods were computationally relatively efficient. Also, they were local, in the sense that the surface-mass density is obtained from observed ellipticities of background galaxies. However, as discussed in ([Seitz et al. 1998](#)), a number of drawbacks were also present:

- While the data needs to be smoothed, objective criteria for how to set the smoothing scale is lacking.
- The quality of the reconstruction is hard to quantify.
- Constraints from additional observables, such as multiple images or arcs⁸, are not easily included.
- The magnification (which is needed to break the so-called mass-sheet degeneracy (to be discussed), is incorporated in a global fashion.

Finally, note also the so-called quadruple method introduced by [Lombardi & Bertin \(1998b\)](#), where the isotropy requirement (25) is replaced by an isotropy requirement on the observable quadrupole moments instead. Note also the works on improving the accuracy of mass reconstruction in various ways ([Lombardi & Bertin 1998a](#); [Lombardi et al. 2002](#)). In [Lombardi & Bertin \(1999\)](#), mass-reconstruction is considered through a variational formulation. The procedure formulated is reported to reduce the relevant execution time by a factor from 100 to 1000 with respect to the fastest methods available at the time.

3.2. Inverse methods for lens-mass reconstruction

The aforementioned issues with the standard KS method, or direct methods more generally, lead to the development of so-called inverse methods, such as maximum-likelihood methods ([Squires & Kaiser 1996](#); [Bartelmann et al. 1996](#)). In the inverse methods, one seeks to fit a very general lens model with the data. One typically parametrizes the lens potential on a grid and then minimizes the regularized log-likelihood function. Take N_g to be the number of galaxies and ϵ_i to denote ellipticity of the i -th galaxy. The shear-likelihood function is then given by ([Schneider et al. 2006](#), Eq. 62)

$$-\ln \mathcal{L} = \sum_{i=1}^{N_g} \frac{|\epsilon_i - g(\boldsymbol{\theta}_i, \psi_n)|^2}{\sigma_i^2(\boldsymbol{\theta}_i, \psi_n)} + 2 \ln(\sigma_i(\boldsymbol{\theta}_i, \psi_n)) + \lambda_e S(\psi_n), \quad (28)$$

where σ_i are standard deviations in the ellipticities, $\boldsymbol{\theta}$ are angular positions and ψ is the discretized potential. The parameter λ_e is a Lagrangian multiplier giving the relative weight of the regularization and the likelihood function. In particular; note that strong-lensing constraints may now be added as Lagrangian multipliers. Thus, in such a formulation of the problem, other types of constraints (e.g. strong lensing and magnification) are more readily included. As an early example, consider [Bartelmann et al. \(1996\)](#) in which

⁸ *Arcllet* seems to be the term used for sheared (stretched) images, whereas the term *arc* is reserved for stronger (flexed) distortions.

magnification constraints are included (to effectively break the mass-sheet degeneracy). The χ^2 -function

$$\chi^2 = \sum_{k,l} \left(\frac{(g_i(k,l) - \mathbf{g}_i(k,l))^2}{\sigma_g(k,l)} + \frac{(r_i(k,l) - \mathbf{r}_i(k,l))^2}{\sigma_r(k,l)} \right) \quad (29)$$

is minimized numerically using a conjugate-gradient method. Here \mathbf{r}_i represents the (inverse) magnification data. The method allows for straight forward inclusion of measurement inaccuracies, and is designed to work well with clusters, where the observed field is small or irregularly shaped. This method was extended by [Seitz et al. \(1998\)](#) to include regularization of the potential and use the individual galaxy ellipticities and positions instead of averaging by dividing the image into cells. [Bridle et al. \(1998\)](#) also includes magnification constraints by a maximum-likelihood approach, here seen as a special case of the maximum-entropy method (MEM) in the context of Bayes' theorem. This method allows for direct reconstruction of the mass distribution instead of going via the gravitational potential.

Other log-likelihood approaches include [Marshall \(2006\)](#), in which an atomic-inference procedure is adopted. Only WL effects are considered, but incorporation of SL effects is reported to be straight forward. Beyond that, the reader is referred to the book-sized review [Bartelmann & Schneider \(2001\)](#) on the early developments of weak gravitational lensing, and weak lensing theory in general.

As we shall see in Section 4, inverse methods have become the standard tool for lens-mass reconstruction. The key factor for its success is its linear problem formulation, where both weak and strong constraints (and others) can be added as linear constraints in a joint analysis.

3.2.1. Degeneracies in the Lens Equation

It was early recognized that the lensing equation suffers from a number of degeneracies, owing to the fact that most observables of gravitational lensing are dimensionless. Early sources on this include [Falco et al. \(1985\)](#) and [Gorenstein et al. \(1988\)](#), written in a time when cluster lenses were still controversial. Later papers, such as [Saha \(2000\)](#) rederives the degeneracies, putting them in a new observational context. Herein, so-called similarity degeneracies are broadly categorized as either a (i) *distance degeneracy* or a (ii) *angular degeneracy*. Another type, the so-called *mass-sheet degeneracy*, also appears for sources at the same redshift⁹. In this case the problem is that the observable distortion, $g = \gamma/(1 - \kappa)$ is invariant under the transformation

$$\kappa \rightarrow (1 - \lambda) + \lambda\kappa, \quad \gamma \rightarrow \lambda\gamma. \quad (30)$$

Globally, this is equivalent to the rescaling

$$\mathcal{A} \rightarrow \lambda\mathcal{A}, \quad \lambda = \text{const.} \neq 0, \quad (31)$$

which leaves the critical curves $\det\{\mathcal{A}\} = 0$ invariant (refer to e.g. [Saha & Williams \(2006\)](#); [Liesenborgs & De Rijcke \(2012\)](#) for more). This means that several source positions may give rise to the same observed position, give and take a mass sheet of constant density. In particular, this transformation keeps the critical curves of the lens mapping fixed, and thus the location of the giant

⁹ Note also the generalization discussed in [Liesenborgs et al. \(2008\)](#)

arcs and arclets. The mass-sheet degeneracy is an example of a broader class of source-plane transformation issues (Schneider & Sluse 2014) for strong lenses. Consequently, since one cannot distinguish between lenses when using distortion data alone (for sources at the same redshift), lens-mass reconstruction algorithms must therefore take measures to break the degeneracy through some means or another. One way to go, would be to use magnification, as tried by Broadhurst et al. (2005); Broadhurst et al. (1994). However, Schneider et al. (2000) points out uncertainties in unlensed source counts, leaving the magnification method less prosperous. Bradač et al. (2004a) sets out to use redshifts instead, and concludes that it is necessary to simultaneously analyse weak and strong lensing to break the mass-sheet degeneracy. Thus it is about time that we give a more formal definition of the difference between the weak and strong lensing regimes.

3.3. The difference between weak and strong lensing

Strong lensing refers to conditions allowing for multiple images of the same source (Congdon & C.R. 2018, Chapter 2). For this to happen, the lens must possess a certain ‘strength’. The divide between weak and strong lensing is arguably somewhat arbitrary, since it is all part of the same underlying physical phenomena. Nevertheless, from the mathematical side one may show that a sufficient¹⁰ requirement for producing several images of a source under the mapping (1) is $\kappa(0) > 1$, a condition known as *supercriticality*. Furthermore, it may be shown that the magnification diverges whenever $\det \mathcal{A} = 0$, producing the characteristic arcs associated with GL. We can infer the following.

- *Strong-lensing data* ($\kappa > 1$): Incorporating multiple imaging and/or critical curves ($\det \mathcal{A} = 0$).
- *Weak-lensing data* ($\kappa < 1$): This means incorporating shear measurements in the analysis, and sometimes flexion (to be discussed). Note that the aforementioned linear regime ($\kappa, \gamma \ll 1$) lies in the weak-lensing regime.

The reason why these effects have been studied separately, is to some extent historical, owing to the methods and sensitivity available. On the one hand you have the rare but visually apparent effect of strong lensing. This effect is visual, and observed as giant luminous arcs, or multiple images. The sensitivity required of the instruments to capture this effect is therefore low compared to that of weak lensing, which must typically be treated statistically over large samples of lensed images. Whereas strong lensing was used for lens-mass estimation already with Zwicky (1937a,b), weak lensing had its dawn in the 90s, as described earlier.

3.4. Beyond shear: Banana or jelly-bean?

The lensing theory described in the beginning of this chapter, hinges on the map given in Eq. (9), with the linearisation given by (10). For infinitesimal beams, a linearisation is warranted, but if one intends to take into account the finitude of the beam, the linearisation breaks down. Put differently: If the shear varies over the cross-section of the image, higher-order effects, such as flexion and second-flexion come into play. First-flexion is a shift in position of the image centroid, whereas second-flexion creates the banana-

looking shape¹¹. The flexion is a second-order¹² effect, and thus weaker than shear in the weak field. On one hand, this could cause problems in detecting it. On the other hand, however, source galaxies are not believed to be intrinsically flexed, which provides an advantage: the flexion generally belongs to the image. One way to quantify the flexion of a lensed image, is by multipole moments, as for instance in the early work Goldberg & Natarajan (2002), in which it is shown how flexion (octopole moment) can be used as a probe of weak-lensing shear fields. Note also later contributions such as Goldberg & Leonard (2007); Okura et al. (2007); Okura et al. (2008). Another way to quantify flexion, is through the shaplets-formalism due to Refregier. This was e.g. used in Goldberg & Bacon (2005), where an inversion-technique based on flexion was investigated, reporting an increased signal-to-noise ratio. In Bacon et al. (2006), the flexion-formalism is tidily presented in complex form, also revealing a spin-3 field which has come to be known as the aforementioned second-flexion. To summarize, one has

$$\mathcal{F} = |\mathcal{F}|e^{i\phi} = \partial\kappa \quad \text{first flexion (spin-1),} \quad (32)$$

$$\mathcal{G} = |\mathcal{G}|e^{i3\phi} = \partial\gamma \quad \text{second flexion (spin-3),} \quad (33)$$

where $\partial = \partial_1 + i\partial_2$ is a complex derivative incorporating the two directions (1, 2) of the screen-space and star denotes complex conjugation. Sometimes \mathcal{F} is referred to as comatic flexion and \mathcal{G} is referred to as trefoil flexion. The flexion has four components, and the relation between the spin-1 and spin-3 components are given by

$$\partial^* \partial \mathcal{G} = \partial \partial \mathcal{F} \quad \text{consistency relation,} \quad (34)$$

which can be readily proven. The paper also calculates the flexion coefficients for various spherical lensing profiles. In Bacon & Schafer (2009) it is also shown how the flexion term arises when one includes the final Pauli spin matrix n . The reader should also note the seemingly independent development of higher-order lensing throughout the papers Irwin & Shmakova (2003); Irwin & Shmakova (2005); Irwin & Shmakova (2006); Irwin et al. (2007), under the name *sexupole* lensing¹³. Although originally intended for galaxy-galaxy-lensing, flexion measurements were already in 2007 performed on the cluster Abell 1689, revealing a dark matter structure that was not apparent from shear measurements alone Leonard et al. (2007). Flexion can also be estimated through the so-called analytic image model (AIM) Cain et al. (2011), and a subsequent study based on this method confirms that significant sub-structures may remain invisible if this effect is not taken into account in cluster lensing Cain et al. (2016). Flexion with elliptical lens profiles is investigated by Hawken & Bridle (2009), where it is found that the constraints on galaxy halo ellipticities are comparable or even up to two orders of magnitude higher than those from shear.

Just like the actual observable of shear γ is the reduced shear g , the actual observable when it comes to flexion is the *reduced flexion*, calculated in Schneider & Er (2008), and tested against simulations. One result is that the presence of flexion affects the determination of the reduced shear. In Er et al. (2010) the problem of cluster

¹¹ or is it a jelly bean?

¹² If we by ‘order’ mean the number of derivatives in a Taylor-expansion.

¹³ This seems to be in contrast to Goldbergs’ notion of flexion as an octopole term.

¹⁰ Sufficient and necessary in the case of axisymmetric lenses. Only sufficient in the more general case.

lens-mass reconstruction is considered, combining strong-lensing constraints with weak-lensing shear and flexion. By so, the weak-lensing analysis is extended to the inner parts of the cluster, and the resolution of substructure improved. Also, [Lasky & Fluke \(2009\)](#) calculates the flexion for a diversity of circularly symmetric lenses, and concludes that the convergence and first-flexion are better indicators of the Sérsic shape parameter, while for the concentration of NFW profiles, the shear and second-flexion terms are preferred. In a follow-up work ([Fluke & Lasky 2011](#)) the ray-bundle-method (RBM) developed in [Fluke et al. \(1999\)](#) is applied and found to accurately recover second-flexion for the Schwarzschild lens. Also, the existence of a preferred flexion zone is demonstrated. The RBM could be described as an attempt at using a strong-lensing approach to weak lensing, by considering the fact that light rays come in bundles, and not as single, infinitesimal rays. The idea of a strong-lensing formalism for weak lensing is furthered by [Fleury et al. \(2017, 2019a,b\)](#). Here the *infinitesimal-beam approximation* underlying weak lensing approaches is found to yield problems. This approximation is shown to comprise the following three approximations:

- *flat-sky-approximation*: Distances are such that the lens and source planes can be approximated by planes.
- *weak-field regime*: The space-time metric can be considered locally flat within the beam’s cross section.
- *Smooth curvature*: The riemann curvature can be considered constant over the beam’s cross section.

By rejecting this approximation and studying instead a finite beam, the authors show that the Kaiser-Squires theorem is violated by finite-size effects.

Another paper, [Birrer et al. \(2017\)](#), seeks to unite the two regimes (weak and strong) by looking at *line-of-sight* (LOS) deflectors in galaxy-scale lensing. In this formalism, the main deflector is a strong deflector, upon which small LOS deflectors are added in a perturbative manner. Strong-lens systems are shown to be accurate and precise probes of cosmic shear.

The converse; a weak-lensing approach to strong lensing is taken in [Clarkson \(2015\)](#), where the general theory of secondary weak gravitational lensing is developed. This approach is later extended to include all leading-order screen-space derivatives [Clarkson \(2016a,b\)](#), as such extending the work by Bacon et al (2006 and 2009) from an altogether different route. This latter extension by Clarkson is referred to as the *roulette formalism*, and for circularly symmetric lenses it is shown to reproduce strong-lensing features. In a later paper recursion relations (/consistency relations) like (34) are developed for the higher-order terms ([Normann & Clarkson 2020](#)) in context of general non-symmetrical lenses. These relations have proven useful in a simulator developed (CosmoAI), with a visualization component [Schaathun et al. \(2023a\)](#), to both showcase the roulette expansion and also to investigate its ability for lens-mass reconstruction [Schaathun et al. \(2023b\)](#). It is noteworthy that the roulette formalism, in its current standing, does not include all terms in the full, non-linear geodesic deviation equation, as described by [Vines \(2015\)](#).

Finally, note also [Lanusse et al. \(2016\)](#), where a mass-mapping algorithm designed to recover small-scale information from a combination of gravitational shear and flexion is developed, starting from the geodesic deviation equation. The reconstruction method is tested on realistic weak-lensing simulations corresponding to typical Hubble-space telescope (HST) / Advanced Camera for studies (ACS)

cluster observations. The inclusion of flexion is found to increase signal-to-noise level on small scales.

It seems fair to conclude that despite difficulties in actually measuring flexion [Viola et al. \(2012\)](#); [Rowe et al. \(2013\)](#), this higher-order effect has proven to be of importance. Although perhaps limited by the current state-of-the-art observational situation, it is natural to wonder if even higher-order terms (Roulette expansion), could prove useful.

3.5. Cluster lenses

The observation of weak lensing by clusters were reported by Tyson, Valdes and Wenk ([Tyson et al. 1990](#)) in a seminal paper, in some sense marking the beginning of observational support for weak lensing. Attempts to determine cluster lens-mass distributions, however, seem to go back to [Webster \(1985\)](#), while [Kochanek \(1990\)](#) and [Miralda-Escude \(1991\)](#) discussed how parameterized cluster-mass distributions could be constrained from weak-lensing data through ellipticities of the source and image. The effects of cluster strong lensing were however first unknowingly discovered when observing giant luminous arcs ([Lynds & Petrosian 1986](#))¹⁴, with subsequent interpretation of the phenomena as a lensing effect ([Soucail et al. 1987](#)).

Whereas a power-law of the form $\rho \sim 1/r^j$ seems to work well for modelling lenses on galactic scale, this does not apply to clusters. A natural generalization would be to allow the power law index to take on one value for small radii and another for large radii, like the Navarro-Frenk-White (NFW) model. Here

$$\rho(r) = \frac{\rho_s r_s^q}{r^p (r_s + r)^{q-p}} \quad \text{NFW profile,} \quad (35)$$

for some scale radius r_s . For $r \ll r_s$ one finds $\rho \sim 1/r^p$, whereas $\rho \sim 1/r^q$ for $r \gg r_s$. From cosmological simulations of cluster-sized dark-matter halos [Navarro et al. \(1995\)](#); [Navarro et al. \(1996\)](#); [Navarro et al. \(1997\)](#) found $p = 1$ and $q = 3$. Later parametric models have often taken this profile as a starting point. Now that the resolution of the image data is increasing, there is however a need for going beyond such parametric models.

3.6. Parametric and non-parametric (free-form) models

For the purpose of this review it is useful to make a distinction between parametric and non-parametric models. We employ the classification from [Lefor et al. \(2013\)](#), where parametric models make assumptions on physical objects (as e.g. point-masses, singular isothermal spheres and so on) to model the lensing mass. While non-parametric (or free-form) models do lens inversion by avoiding such assumptions and rely on the lensed images alone to do mass reconstruction. In the non-parametric approach several models can fit the observed data, and a regularization problem needs to be solved to restrict results to plausible surface-mass densities. An example of a non-parametric approach that created some stir is [Jee et al. \(2007\)](#), where a dark-matter ring in the cluster CL0024+17 ($z = 0.395$) was discovered, using both strong and weak lensing constraints. When using non-parametric models, a large number of constraints is needed to avoid spurious results, as discussed

¹⁴ Zwicky also considered clusters, but at this stage in the development shift in position was the discussed effect.

for instance in Ponente & Diego (2011) and Sendra et al. (2014).

Abell1689 is a good example of a cluster where non-parametric models are competitive with parametric ones, since there are so many constraints (hundreds of arcs). Parametric models are typically popular in the inner parts of clusters, where the lensing effects are strong. In practice, a combination of both parametric and free-form modelling is used, such as e.g. in Jullo & Kneib (2009) and in Beauchesne et al. (2021).

4. Cluster lens-mass reconstruction from weak- and strong lensing combined

The treatment so far has been general, giving the development of weak lensing theory beyond shear (id est towards the strong regime) and by explaining important concepts and issues. Furthermore, the turn to maximum-likelihood methods (discussed in Sec. 3.2) was an important step, which the community continued to develop from Bridle and on. With it, both weak and strong constraints could be jointly analysed through linear constraints.

In the current section we narrow in to cluster lens-mass reconstruction, and review the development of methods for unified analysis. The shortlist from the systematic review (cf. discussion in Section 2) makes up the bulk of material covered.

4.1. Weak lensing (arcllets) combined with multiple images

The strong lensing regime permits for multiple images of the same source. Such information may be used for lens-mass reconstruction, as investigated by numerous sources, such as e.g. AbdelSalam et al. (1998c). This particular work by Abdel Salam et al, however, is furthered in a series of papers to include also weak-lensing information for cluster lens-mass reconstruction (AbdelSalam et al. 1997, 1998a; Saha et al. 1999). The technique developed uses constraints from multiple images and arcllets. The technique bears resemblance with that of Kaiser & Squires (1993) for weak lensing, but this time the problem formulation is *linear*: The aforementioned strong-lensing constraints are included as linear constraints on the projected mass distribution, together with weak-lensing constraints. Quadratic programming is then used to obtain the mass maps, and the method developed is reported to overcome the drawbacks of non-linear methods, such as the mass-sheet degeneracy (by using sources at different redshifts), and the technique is also applied to cluster lens-mass reconstruction (see also AbdelSalam et al. (1998b)).

Another early example is Kneib et al. (2003), which studies the particular cluster C1 0024+1654 ($z = 0.395$). The study imcorporates strong-lensing constraints (multiple images) in a weak-lensing analysis, using the maximum-entropy method developed in Bridle et al. (1998). The strong-lensing constraints are found to narrow down the parameter space effectively, with an analysis strongly rejecting the SIS model, whilst fitting that of an NFW profile well. A shortcoming of the study is that it is not parameter-free. Also, the parametrization only allows weak-lensing signals in the outer parts (~ 570 kpc) and strong lensing constraints from the inner regions (155 kpc). In Smith et al. (2005) the software LENSTOOL is used together with additional routines to incorporate weak-lensing constraints. Again the algorithm used builds on parametric

models, with a χ^2 -estimator quantifying how well each trial lens model fits the data.

With these works in mind, it therefore seems fair to conclude that around the dawn of the 21th century, the theory was sufficiently mature and observations crisp enough for a joint analysis of both weak and strong lensing constraints. For it is one thing to theoretically being able to perform joint analysis, and quite another to implement it with actual observations. As that step was overcome, however, combining the two regimes is quickly confirmed to be beneficial. But a number of theoretical problems remained however in need of closer attention: (i) The mass-sheet degeneracy must be broken for any study relying on the lens equation, (ii) likelihood methods must be properly regularized and (iii) non-parametric models should be developed.

4.2. Bradač, Umetsu and mass-sheet degeneracy

As already discussed (cf. Sec. 3.2.1), attempts had been made to overcome the mass-sheet degeneracy, which also became an issue in terms of discriminating between the SIS and the NFW profile — a hot topic in connection with cluster lenses. In 2004, Bradač et al published a paper on the mass-sheet degeneracy Bradač et al. (2004a), suggesting a way to break it by using the distortion and the redshift information of background galaxies. They conclude that the method is effective for critical clusters only (multiple imaging). Consequently, in order to break the degeneracy with the current (2004) data, it was found necessary to extend the statistical lensing analysis closer to the cluster center, performing a joint weak and strong lensing analysis. An overview of the results is presented in a proceedings (Bradač et al. 2004b), with reference to further literature, alongside an implementation with the cluster-mass distribution of RX J1347-1145. The method developed is again parametric, and in Bradač et al. (2004a) attention is called to non-parametric models, since the method in principle should be applicable in such scenarios as well. Consequently, in a series of papers, Bradač et al propose a non-parametric method for uniting weak and strong lensing (Bradač et al. 2005; Bradač 2005), accompanied by observational implementations (Bradač et al. 2005, 2006; Bradač et al. 2005a). The method relies on minimizing the χ^2 functional

$$\chi^2(\psi_k) = \chi_{\text{WL}}^2(\psi_k) + \chi_{\text{MI}}^2(\psi_k) + \eta R(\psi_k), \quad (36)$$

where subscripts WL and MI denote weak lensing and multiple imaging, respectively. ψ_k is the lensing potential on a regular grid, whereas the final term is a regularisation term. A minimum is sought such that

$$\partial\chi^2(\psi_i)/\partial\psi_i = 0. \quad (37)$$

The authors comment on the fact that other attempts at combining weak and strong lensing have already been made. For instance, they point out that Abdelsalam et al and Smith et al (Sec. 4.1) use the surface-mass density κ , on which the shear γ and the deflection angle α depends non-locally. Bradač et al uses instead the potential ψ , from which both convergence, shear and the deflection angle may be locally derived (derivatives). Where Kneib et al (2003) and Smith et al (2004) (cf. Sec. 4.1) used a parametrized, Bayesian approach, a more general parametrization was used by Bradač et al. In 2009 they apply their techniques on the Bullet cluster, with a strong and weak lensing analysis following the algorithm first proposed by Bartelmann et al (1996) and discussed in Sec. 3.2.

Another interesting strand of work, based on the authors original idea of using magnification to break the mass-sheet degeneracy [Broadhurst et al. \(2005\)](#), is also further developed (cf. e.g. [Umetsu & Broadhurst \(2008\)](#); [Medezinski et al. \(2007\)](#); [Umetsu et al. \(2011\)](#)). Finally, in [Umetsu \(2013\)](#), a model-free reconstruction method is presented, using multiple populations of background sources, correcting for magnification bias and incorporating strong-lensing constraints. The method is applied to a number of clusters from the Subaru images.

4.3. Perturbative approach

Another interesting approach within the framework of maximum-likelihood approaches, is the perturbative approach undertaken in [Natarajan et al. \(2009\)](#). Again weak and strong is combined as linear constraints in a maximum-likelihood manner. Galaxy-galaxy lensing in the cluster CL 0024+16 at $z = 0.39$ is used to track the fate of dark-matter subhalos. The gravitational potential is modelled such that

$$\phi_{\text{tot}} = \sum_n \phi_s + \sum_i \phi_{p_i}, \quad (38)$$

where the two ϕ_s ($n = 1$ and $n = 2$) components represent smooth large-scale components, whereas the galaxy subhalo components ϕ_{p_i} are treated as perturbers. The reason for having two large-scale components, is that earlier studies reveal this to be the best-fit model for that particular cluster. Thus this is taken as a prior in the current study, two. The results provide strong support for the tidal-stripping hypothesis.

4.4. Diego et al and the regularization problem

Due to scarce observations, parametric models were initially popular, and superior to non-parametric ones, where the freedom in the models must be regularized – a process that either requires parameteres or a large number of constraints. As observations increased in amount and accuracy, however, constraints from weak and strong lensing combined made such models competitive with parametric ones. This seems to have accelerated the combinations of the two lensing regimes (WL and SL). In addition to the work by [Bradač](#) (previos section) and also that by [Broadhurst \(Broadhurst et al. \(2005\)\)](#) discussed in Sec. 3.2, the work of combining the two regimes was furthered by [Diego et al. \(2007\)](#) in a paper known as Paper III in a series. The work centers around the idea of expanding the projected cluster-mass distribution into a set of basis functions which are then constrained individually using shear and SL data.

Again a maximum-likelihood approach is taken, well suited for the task of combining different types of constraints. Their discretized problem formulation is as follows. Take N_θ to be the number of images, N_s the number of sources and let N_c denote the number of mass cells. Then the linearised problem takes the form

$$\phi = \Gamma \mathbf{x}, \quad (39)$$

where Γ is a matrix of dimension $4(N_\theta) \times (N_c + 2N_s)$, and generally not invertible. ϕ is a vector containing position and shear information whereas \mathbf{x} is a vector containing all the unknowns. A weakness of the work is that it assumes the source galaxies to be point-like¹⁵. This is however corrected

for in an a-posteriori manner, by allowing for residuals \mathbf{r} in the lens equation; $\mathbf{r} = \phi - \Gamma \mathbf{x}$. Approximate solutions to the problem is sought by maximizing the functional $\mathcal{L} = e^{-\frac{1}{2}\chi^2}$, assuming \mathbf{r} is Gaussian. The χ^2 is now defined as

$$\chi^2 = \mathbf{r}^T \mathbf{C}^{-1} \mathbf{r} \quad (40)$$

where \mathbf{C} is the covariance matrix of \mathbf{r} . As with most studies combining weak and strong, this work only includes shear.

Since the approach is non-parametric, a regularization procedure is necessary. In Paper I ([Diego et al. 2005a](#)) a bi-conjugate gradient method minimizing χ^2 , stopping at a target value ϵ is found useful (implicitly regularizing the problem). Paper III shows that combining weak and strong lensing makes the choice of ϵ less relevant. Also, since the problem formulation consists in minimizing a quadratic function with linear constraints, a quadratic-programing approach (QADP) is taken. By using a minimization algorithm that is constrained to minimize χ^2 for positive masses, unphysical negative masses are avoided, and the problem is more properly regularized. An application using strong lensing is found in their Paper II ([Diego et al. 2005b](#)). The result of their analysis is a software package known as WSLAP¹⁶, which is made available for public use. Also note [Diego \(2014\)](#).

The above works illustrate the capability of non-parametric methods to compete with parametric ones, when a properly regularized maximum-likelihood approach is taken.

4.5. Using critical curves

As discussed in Sec. 3.3, strong lensing observables include arcs, which form around critical curves ($\det \mathcal{A} = 0$). This is used in [Cacciato et al. \(2006\)](#) to develop a cluster-potential reconstruction method relying on critical-curve constraints imposed near arc-forming regions. Building on the least- χ^2 minimisation procedure developed in [Bartelmann et al. \(1996\)](#); [Seitz et al. \(1998\)](#), this becomes a different route to combining weak and strong lensing. Also note that the weak-lensing constraints are imposed on a low-resolution grid, whereas the strong-lensing constraints are imposed on a more fine-grained grid, so as to concentrate the analysis to the relevant region.

One advantage of this method, is the elimination of the need to finding multiple images of the same source, which requires work. Additionally, one ought also know whether or not there are additional sources not imaged. But inverting the lens equation to find out is of course a highly non-linear process. Furthermore, multiple imaging is caused by sources inside or close to caustics, which limits the applicability of the method.

In [Cacciato et al \(2006a\)](#) measured ellipticities is compared to γ rather than to the reduced shear $\gamma(1 - \kappa)^{-1}$. This approximation is fixed in the observational follow-up ([Merten et al. 2009](#)), which also improves the gridding of the data, and adds a regularization term to not overfit noise. Note also the follow-up [Merten \(2016\)](#), which incorporates a mesh-free, free-form approach to lens-mass reconstruction, through the use of radial basis functions. When discretizing the data, a regular mesh is often employed. But, as the authors argue, astronomical data is often quite irregular. The work extends their own previous work, and other, like [Bartelmann et al. \(1996\)](#); [Seitz et al. \(1998\)](#);

¹⁵ The paper includes a remark about a follow-up work on this issue, which we have not been able to find.

¹⁶ Weak & Strong Lensing Analysis Package

Bradac et al. (2005b) into the flexible, numerical mesh-free domain.

4.6. Particle-based lensing (PBL)

Let us also make mention of the works Deb et al. (2008, 2012), where a particle-based approach is taken. Whereas grid-based techniques are often optimized to measure at a single scale, reality is that the structure of a cluster lens is hierarchical. Thus a method capable of increased resolution in regions high on information would be desirable. Second, the smoothing and weighting are arguable *ad hoc* by construction (motivated by model and theory), whereas an ideal smoothing scale should be variable. Another point is the abrupt switch in image parity at the critical curves, leading to a discontinuity in the ellipticity as a function of κ and γ . This prevents linear minimization schemes from converging to a "strong lens"-solution if starting off by a "weak lens" initial guess.

The particle-based lensing (PBL) methods has the ability to combine disparate lensing scales in a coherent way without regularization schemes, and are already in use in other fields of astrophysics where a wide range of physical scales are present, such as numerical N -body simulations.

PBL is a new way of discretizing and describing a reconstructed field, including a metric comparison to the observed data, but PBL is nevertheless not a minimization scheme. PBL consists of a list of potentials (one at each observed lensed image) and a metric to describe the goodness of fit. A χ^2 minimization to estimate a maximum-likelihood potential field is used, and—for practical implementations anyway—some sort of minimization procedure has to be chosen.

Note that the (parameter free) PBL method developed may in principle combine both weak and strong constraints, including flexion. Applying the technique to the much studied cluster CL-A1689 reveals a secondary mass peak in the north-east direction, confirming previous optical observations Deb et al. (2012). The study is reported to be the first non-parametric strong and weak (shear) mass map with a covariance matrix. Also see Deb et al. (2010) for another application of PBL to lensing, and for more on the covariance matrix.

4.7. Including flexion in the combined analysis

Including flexion, the lensing equation may be written as Cain et al. (2011)

$$\hat{\beta} = \theta - g\theta^* - \frac{1}{4}\Psi_1^*\theta^2 - \frac{1}{2}\Psi_1\theta\theta^* - \frac{1}{4}\Psi_3(\theta^*)^2, \quad (41)$$

where θ is the complexified image-plane angular coordinate and $*$ denotes complex conjugation. Note that $\hat{\beta} = \beta/(1 - \kappa)$ is the reduced source position, g is the reduced shear, as before (17), and that $\Psi_1 = \frac{\mathcal{F}}{1 - \kappa}$ and $\Psi_3 = \frac{\mathcal{G}}{1 - \kappa}$ are reduced flexion variables (cf. Eq. (32)), all fit to taking the mass-sheet degeneracy into account.

It is in fact notable that weak lensing including flexion terms has also been combined with strong lensing constraints in observational studies, as described in this section. First, note the study Leonard et al. (2007), where shaplets are used. Again the cluster Abell1689 is the target cluster. By use of flexion-data alone, and with a parametric approach, the study reveals a substructure offset from the central cluster members that was not visible from shear measurements alone. With non-parametric approach it is

also suggested, by combination of weak and strong lensing data. Several studies show the same; flexion is particularly sensitive to cluster substructures (e.g. Bacon et al. (2010)). This is perhaps not so surprising from a theoretical point of view, considering the fact that flexion encodes derivatives of the shear map.

The mass-reconstruction method presented by Bradac and discussed earlier, is extended in Er et al. (2010), where a flexion term χ_f^2 is added, reading

$$\sum_{i=1}^{N_f} = \frac{|t_{1i} - G_1(\theta_i, z_i)|^2}{\sigma_{i1}^2} + \frac{|t_{3i} - G_3(\theta_i, z_i)|^2}{\sigma_{i3}^2}, \quad (42)$$

where t_{1i} (or t_{3i}) refers to first (or third) flexion data, and G_{1i} (or G_{3i}) to the corresponding theoretical model flexion. N_f is the number of images with flexion data. The approach is tested on simulations, and concludes that flexion is sensitive to sub structures.

Also note the Analytic Image Model (AIM) method, developed in Cain et al. (2011), which is distinct from shaplets- and moment-based methods. Starting from the conservation of surface-brightness $I_{\text{obs}}[\theta] = I_{\text{src}}[\beta(\theta)]$, it minimizes the figure of merit given by

$$\chi^2 = \sum_n \frac{(I_{\text{obs}}(\theta^{(n)}) - I_{\text{AIM}}(\theta^{(n)}; p_{\text{int}}, p_{\text{lens}})^2)}{\sigma_n^2}, \quad (43)$$

where $\theta^{(n)}$ is the image-plane position of the n th pixel and σ_n^2 is an estimate of the variance in that pixel's value. Note that p_{int} and p_{lens} are arrays containing the parameters of the theory. In particular, $p = \{g_1, g_2, \Psi_{11}, \Psi_{12}, \Psi_{31}, \Psi_{32}\}$, where g_1, Ψ_{11} and Ψ_{31} are the real parts (and g_2, Ψ_{12} and Ψ_{32} are the imaginary parts) of g, Ψ_1 and Ψ_3 , respectively. Instead of estimating derived quantities, such as shapelet coefficients or surface-brightness moments, the AIM method instead fits a mass-sheet transformation invariant model to each galaxy image. The method is applied to CL—A1689, detecting mass structures. In a follow-up work Cain et al. (2016), the AIM method is applied to clusters, revealing that galaxy-group scale substructures may remain undetected, such as to underestimate the mass in such regions by $\sim 25 - 40$ percent. With flexion included, subhalo masses of $\sim 3 \times 10^{12} M_\odot$ are detectable at an angular resolution smaller than 10 arcsec.

Albeit not including strong lensing events per say, we also mention Lanusse et al. (2016), which combines weak-lensing shear and flexion data through developing a method that avoids any binning of the irregularly sampled fields. As a result, the mass-mapping problem becomes an ill-posed inverse problem. This is regularized using a robust multi-scale wavelet sparsity prior. Fast Fourier estimators makes the algorithm efficient, and the method is tested on simulated data. The conclusion is again that flexion increases the ability to detect substructures.

4.8. Combining lensing information with other sources

In this paper we have focused on gravitational lensing as a probe on galaxy clusters. But there are other probes as well, which may be summarised as follows:

- weak and strong lensing constrain the line-of-sight projection of the cluster potential
- X-ray observations constrain the density and the temperature of the intracluster gas
- Sunyaev-Zeldovich effect constrains the gas pressure

- Gradient of gravitational potential can be constrained by galaxy kinematics
- Cluster kinematics. In e.g. Pizzuti et al. (2022) kinematics measurements of galaxy cluster MACS J1206 is combined with weak and strong lensing constraints.

A complete treatment would of course have to combine from all the above approaches. Although alternative sources for information is beyond the scope of the current review, we take the opportunity to mention that work has been done in combining the available information. One example is Konrad et al. (2013), where reconstruction from thermal gas (x-ray) and gravitational lensing is considered in a non-parametric manner. The ultimate goal of this study is reported to be a non-parametric method combining strong and weak lensing, observations of thermal gas physics, and galaxy kinematics into one consistent model for the projected cluster potential. Other examples include Majer et al. (2016) where lensing information is combined with the thermal Sunyaev-Zel'dovich effect and Tchernin et al. (2015, 2018), where X-ray and the Sunyaev-Zel'dovich effect is used to reconstruct the gravitational potential by joint analysis.

4.9. Software developments

As far as software goes, the recently developed Niemiec et al. (2020), should be noted, where the combination of weak and strong constraints are implemented in the publically available modelling software package LENSTOOL, and called *hybrid*-LENSTOOL. The name derives from the process: This package uses a parametric approach to model the core of the cluster, and a non-parametric (free-form) approach for the outskirts. The optimization is based on a joint optimization of both weak and strong constraints, such that the combined likelihood function is

$$\mathcal{L}(\Theta, w) = \mathcal{L}_{\text{SL}}(\Theta, w) \times \mathcal{L}_{\text{WL}}(\Theta, w). \quad (44)$$

Here Θ are the free parameters of the parametric part, whereas the grid model composed of N radial basis functions are ordered in a vector w . The details of the strong- and weak-lensing likelihoods are further described in the paper. As a result, the package optimizes weak- and strong lensing simultaneously, as opposed to successively, as does the fore-runner *Sequential-Fit*. It should be noted, however, that Niemiec et al. (2023) still ends up using *Sequential fit*, since the strong lensing constraints optimizes the likelihood in the source plane, as opposed to the image plane. This might not be accurate enough for complex clusters, given that best-fit mass reconstruction is the goal. Testing both methods on simulated clusters are left for future work. Another software is SWUnited, based on the Bradac-Hoag model. This algorithm is based on the works Bartelmann et al. (1996) (Sec. 3.2) and Bradac et al. (2005) (Sec. 4.2), is non-parametric (free-form) and reconstructs the lensing potential (as opposed to the convergence). This means that assumptions on the mass density outside the field of observation is not necessary. Also, the formalism includes flexion constraints.

Note also WSLAP+, which builds on work by Diego (discussed in Section 4.4) and Lam. This method also unites strong and weak (shear) constraints.

A genetic algorithm (GA) for non-parametric strong-lensing systems (GRALE) was also developed (Liesenborgs et al. (2007); Liesenborgs et al. (2010)),

and later extended to take time-domain and weak-lensing information into account (Liesenborgs et al. 2020). This method resembles a regularization procedure, but is different in that it does not optimize the different criteria together. Instead, a GA looks for a common optimum for the different so-called fitness measures. The results as regards the addition of weak lensing to GRALE¹⁷, are reported to be somewhat mixed, and the procedure is plagued by the mass-sheet degeneracy.

Finally, note also the newly developed RELENSING package (Torres-Ballesteros & Castañeda 2023), written in Python. It is a free-form approach on an adaptive, irregular grid, combining strong and weak (shear) constraints, and tested on the simulated clusters ARES and HERA.

A full analysis and comparison of (some of) the different packages available shall not be undertaken here, but we refer the interested reader to Meneghetti et al. (2017), where different groups have participated in the reconstruction of simulated clusters, for comparison purposes. Other tests include the Shear TEsting Programme (STEP) and GRAvitational LEnsing Accuracy Testing (GREAT).

4.9.1. The use of artificial intelligence

As a final remark, it is worthwhile stopping to ponder the future. As numerous authors point out, the amount and quality of the lensing data has been steadily increasing. Resultingly, one ought only expect that the need for fast, automated analysis becomes more and more prevalent. To this end, people have looked to machine learning, to see if this tool is fit for the job of automating the process of lens-mass reconstruction. Novel attempts have been made, such as that by Hezaveh et al. (2017), Galan et al. (2022) and Biggio et al. (2023), all concerning strong lenses. To the best of knowledge, no other attempts at combining weak and strong lensing in an automated ML approach has been made, besides our own humble attempt at using the Roulette formalism to such ends Schaathun et al. (2023a,b), and the recent work by Cha et al. (2024), where a deep-learning technique is applied to navigate the extremely large space of free parameters. The data set of this latter study is obtained from wide-field JWST, which makes it all the more interesting. As mentioned, however, this is beyond the scope of this review, and should be treated elsewhere.

5. Conclusion and future outlook

In this review, we have traced the development of joint analysis of weak and strong gravitational lensing data, with a particular emphasis on cluster lens-mass reconstruction. In summary there seems to be two important strands of development.

First, there is the development of the theory of weak lensing to account for higher-order terms, such as flexion, second-flexion and terms beyond (so-called roulette expansion). This is a natural extension of the early development of non-linear methods (such as KS). By including terms beyond shear in the lens map a bridge is made from the weak regime towards the strong. As of today, the roulette expansion developed by Clarkson is the most complete work to this end, but even here only leading-order screen-space terms have been kept, whereas the rest, such as line-of-sight effects, are wittingly swept under the carpet.

¹⁷ Short for GRAvitational Lenses.

Second, with the development of so-called inverse methods (and most prominent among them the class of maximum-likelihood approaches) around the turn of the millennium, the two regimes have arguably been merged, as far as statistical data analysis is concerned. However, a number of improvements are possible. In weak studies, inclusion of flexion terms has already proven useful, but terms beyond this order have not been investigated, except theoretically in the aforementioned roulette formalism, or equivalently, by Fleury et al. Foreseeing an increase in data quality, such decomposition of image information beyond flexion could prove valuable.

Future work

A number of improvements are possible. For one, degeneracies such as the mass-sheet degeneracy still plague the field, even in the presence of source red-shift information, and the development of alternative methods thus seems useful. Work on adaptive grids and alternative sources of information to break the degeneracy should therefore be continued.

Flexion studies, adaptive grids and combined analysis of weak and strong lensing have revealed sub-structures in cluster-mass distributions. The development of three-dimensional parametric models of clusters should therefore go on, reaching beyond the NFW. To such ends, studying the line-of-sight effects from the internal structure of the lens seems to be a natural step. Furthermore, the development of non-parametric methods for data fitting must continue, adapting to the increase in both data quality and quantity.

To this end the recent developments within automated processes by use of machine learning seems like a particularly promising route. Armed with a formalism capable of drawing information beyond shear in the so-called weak-lensing data, this might be just what we need.

Acknowledgements. We thank Elise Lindegaard Hanssen for valuable comments.

References

- AbdelSalam, H. M., Saha, P., & Williams, L. L. 1998a, *New Astronomy Reviews*, 42, 157, gravitational Lensing: Nature's Own Weighing Scales
- AbdelSalam, H. M., Saha, P., & Williams, L. L. 1998b, *The Astronomical Journal*, 116, 1541
- AbdelSalam, H. M., Saha, P., & Williams, L. L. R. 1997, *Cluster Mass Profile from Lensing*
- AbdelSalam, H. M., Saha, P., & Williams, L. L. R. 1998c, *Monthly Notices of the Royal Astronomical Society*, 294, 734
- Bacon, D. J., Amara, A., & Read, J. I. 2010, *Monthly Notices of the Royal Astronomical Society*, 409, 389–395
- Bacon, D. J., Goldberg, D. M., Rowe, B. T. P., & Taylor, A. N. 2006, *Monthly Notices of the Royal Astronomical Society*, 365, 414
- Bacon, D. J. & Schafer, B. M. 2009, *Monthly Notices of the Royal Astronomical Society*, 396, 2167
- Bartelmann, M. 1995, *A&A*, 303, 643
- Bartelmann, M., Narayan, R., Seitz, S., & Schneider, P. 1996, *ApJ*, 464, L115
- Bartelmann, M. & Schneider, P. 2001, *Phys. Rep.*, 340, 291
- Beauchesne, B., Clément, B., Richard, J., & Kneib, J.-P. 2021, *Monthly Notices of the Royal Astronomical Society*, 506, 2002
- Biggio, L., Vernardos, G., Galan, A., Peel, A., & Courbin, F. 2023, *Astronomy & Astrophysics*, 675, A125
- Birrer, S., Welschen, C., Amara, A., & Refregier, A. 2017, *Journal of Cosmology and Astroparticle Physics*, 2017, 049
- Bradac, M. 2005, *PoS*, 014
- Bradač, M., Clowe, D., Gonzalez, A. H., et al. 2006, *The Astrophysical Journal*, 652, 937
- Bradac, M., Erben, T., Schneider, P., et al. 2005, *Astronomy & Astrophysics*, 437, 49
- Bradač, M., Erben, T., Schneider, P., et al. 2005, *Astronomy & Astrophysics*, 437, 49
- Bradač, M., Lombardi, M., & Schneider, P. 2004a, *Astronomy & Astrophysics*, 424, 13
- Bradač, M., Schneider, P., Erben, T., & Lombardi, M. 2004b, *Proceedings of the International Astronomical Union*, 2004, 155
- Bradac, M., Schneider, P., Erben, T., & Lombardi, M. 2005a, in *Gravitational Lensing Impact on Cosmology*, Vol. 225, 155–160
- Bradac, M., Schneider, P., Lombardi, M., & Erben, T. 2005b, *Astronomy & Astrophysics*, 437, 39
- Bradač, M., Schneider, P., Lombardi, M., & Erben, T. 2005, *Astronomy & Astrophysics*, 437, 39
- Bradač, M., Treu, T., Applegate, D., et al. 2009, *The Astrophysical Journal*, 706, 1201
- Bridle, S. L., Hobson, M. P., Lasenby, A. N., & Saunders, R. 1998, *Monthly Notices of the Royal Astronomical Society*, 299, 895
- Broadhurst, T., Takada, M., Umetsu, K., et al. 2005, *ApJ*, 619, L143
- Broadhurst, T. J., Taylor, A., & Peacock, J. 1994, *arXiv preprint astro-ph/9406052*
- Cacciato, M., Bartelmann, M., Meneghetti, M., & Moscardini, L. 2006, *Astronomy & Astrophysics*, 458, 349
- Cain, B., Bradač, M., & Levinson, R. 2016, *Monthly Notices of the Royal Astronomical Society*, 463, 4287
- Cain, B., Schechter, P. L., & Bautz, M. W. 2011, *ApJ*, 736, 43
- Cha, S., HyeonHan, K., Scofield, Z. P., Joo, H., & Jee, M. J. 2024, *Astrophys. J.*, 961, 186
- Clarkson, C. 2015, *Journal of Cosmology and Astroparticle Physics*, 2015, 033
- Clarkson, C. 2016a, *Classical and Quantum Gravity*, 33
- Clarkson, C. 2016b, *Classical and Quantum Gravity*, 33
- Congdon, A. & C.R., K. 2018, *Principles of Gravitational Lensing*, 1st edn. (Springer-Cham), XIII, 287
- Deb, S., Goldberg, D. M., Heymans, C., & Morandi, A. 2010, *ApJ*, 721, 124
- Deb, S., Goldberg, D. M., & Ramdass, V. J. 2008, *The Astrophysical Journal*, 687, 39
- Deb, S., Morandi, A., Pedersen, K., et al. 2012, *arXiv preprint arXiv:1201.3636*
- Diego, J. 2014, in *Proceedings of the 49th Rencontres de Moriond on Cosmology*
- Diego, J., Protopapas, P., Sandvik, H., & Tegmark, M. 2005a, *Monthly Notices of the Royal Astronomical Society*, 360, 477
- Diego, J., Sandvik, H., Protopapas, P., et al. 2005b, *Monthly Notices of the Royal Astronomical Society*, 362, 1247
- Diego, J., Tegmark, M., Protopapas, P., & Sandvik, H. 2007, *Monthly Notices of the Royal Astronomical Society*, 375, 958
- Er, X., Li, G., & Schneider, P. 2010, *arXiv preprint arXiv:1008.3088*
- Falco, E., Gorenstein, M., & Shapiro, I. 1985, *The Astrophysical Journal*, 289, L1
- Fleury, P., Larena, J., & Uzan, J. P. 2017, *Physical Review Letters*, 119
- Fleury, P., Larena, J., & Uzan, J.-P. 2019a, *Physical Review D*, 99
- Fleury, P., Larena, J., & Uzan, J.-P. 2019b, *Physical Review D*, 99
- Fluke, C. J. & Lasky, P. D. 2011, *Monthly Notices of the Royal Astronomical Society*, 416, 1616
- Fluke, C. J., Webster, R. L., & Mortlock, D. J. 1999, *MNRAS*, 306, 567
- Galan, A., Vernardos, G., Peel, A., Courbin, F., & Starck, J.-L. 2022, *Astronomy & Astrophysics*, 668, A155
- Goldberg, D. M. & Bacon, D. J. 2005, *Astrophysical Journal*, 619, 741
- Goldberg, D. M. & Leonard, A. 2007, *The Astrophysical Journal*, 660, 1003–1015
- Goldberg, D. M. & Natarajan, P. 2002, *The Astrophysical Journal*, 564, 65
- Gorenstein, M. V., Falco, E. E., & Shapiro, I. I. 1988, *ApJ*, 327, 693
- Hawken, A. J. & Bridle, S. L. 2009, *MNRAS*, 400, 1132
- Hezaveh, Y. D., Levasseur, L. P., & Marshall, P. J. 2017, *Nature*, 548, 555
- Irwin, J. & Shmakova, M. 2005, *New Astronomy Reviews*, 49, 83, sources and Detection of Dark Matter and Dark Energy in the Universe
- Irwin, J. & Shmakova, M. 2006, *ApJ*, 645, 17
- Irwin, J., Shmakova, M., & Anderson, J. 2007, *ApJ*, 671, 1182
- Irwin, J. & Shmakova, M. V. 2003, in *American Astronomical Society Meeting Abstracts*, Vol. 203, American Astronomical Society Meeting Abstracts, 120.06
- Jauzac, M., Jullo, E., Kneib, J.-P., et al. 2012, *Monthly Notices of the Royal Astronomical Society*, 426, 3369
- Jee, M. J., Ford, H. C., Illingworth, G. D., et al. 2007, *ApJ*, 661, 728
- Jullo, E. & Kneib, J.-P. 2009, *Monthly Notices of the Royal Astronomical Society*, 395, 1319
- Kaiser, N. & Squires, G. 1993, *Astrophysical Journal*, 404, 441
- Kaiser, N., Squires, G., & Broadhurst, T. 1995, *Astrophysical Journal*, 449, 460
- Kneib, J.-P., Hudelot, P., Ellis, R. S., et al. 2003, *The Astrophysical Journal*, 598, 804

- Kochanek, C. S. 1990, *Monthly Notices of the Royal Astronomical Society*, 247, 135
- Konrad, S., Majer, C. L., Meyer, S., Sarli, E., & Bartelmann, M. 2013, *Astronomy & Astrophysics*, 553, A118
- Lanusse, F., Starck, J. L., Leonard, A., & Pires, S. 2016, *A&A*, 591, A2
- Laplace, S. 1795
- Lasky, P. D. & Fluke, C. J. 2009, *Monthly Notices of the Royal Astronomical Society*, 396, 2257
- Lefor, A. T., Futamase, T., & Akhlaghi, M. 2013, *New Astronomy Reviews*, 57, 1
- Leonard, A., Goldberg, D. M., Haaga, J. L., & Massey, R. 2007, *ApJ*, 666, 51
- Liesenborgs, J. & De Rijcke, S. 2012, *MNRAS*, 425, 1772
- Liesenborgs, J., de Rijcke, S., & Dejonghe, H. 2010, GRALE: A genetic algorithm for the non-parametric inversion of strong lensing systems, *Astrophysics Source Code Library*, record ascl:1011.021
- Liesenborgs, J., De Rijcke, S., Dejonghe, H., & Bekaert, P. 2007, *Monthly Notices of the Royal Astronomical Society*, 380, 1729
- Liesenborgs, J., De Rijcke, S., Dejonghe, H., & Bekaert, P. 2008, *Monthly Notices of the Royal Astronomical Society*, 386, 307
- Liesenborgs, J., Williams, L. L., Wagner, J., & De Rijcke, S. 2020, *Monthly Notices of the Royal Astronomical Society*, 494, 3253
- Lombardi, M. & Bertin, G. 1998a, *A&A*, 335, 1
- Lombardi, M. & Bertin, G. 1998b, *A&A*, 330, 791
- Lombardi, M. & Bertin, G. 1999, *A&A*, 348, 38
- Lombardi, M., Schneider, P., & Morales-Merino, C. 2002, *Astronomy & Astrophysics*, 382, 769–786
- Lynds, R. & Petrosian, V. 1986, in *Bulletin of the American Astronomical Society*, Vol. 18, 1014
- Majer, C., Meyer, S., Konrad, S., Sarli, E., & Bartelmann, M. 2016, *Monthly Notices of the Royal Astronomical Society*, 460, 844
- Marshall, P. 2006, *Monthly Notices of the Royal Astronomical Society*, 372, 1289
- Medezinski, E., Broadhurst, T., Umetsu, K., et al. 2007, *ApJ*, 663, 717
- Meneghetti, M., Natarajan, P., Coe, D., et al. 2017, *MNRAS*, 472, 3177
- Merten, J. 2016, *Monthly Notices of the Royal Astronomical Society*, 461, 2328
- Merten, J., Cacciato, M., Meneghetti, M., Mignone, C., & Bartelmann, M. 2009, *Astronomy & Astrophysics*, 500, 681
- Miralda-Escude, J. 1991, *Astrophysical Journal*, 380, 1
- Miralda-Escude, J. 1991, *ApJ*, 370, 1
- Mitchell, J. 1784, *Philosophical Transactions of the Royal Society of London (1776-1886)*, 74
- Morandi, A., Pedersen, K., & Limousin, M. 2011, *The Astrophysical Journal*, 729, 37
- Natarajan, P., Kneib, J.-P., Smail, I., et al. 2009, *The Astrophysical Journal*, 693, 970
- Navarro, J. F., Frenk, C. S., & White, S. D. M. 1995, *MNRAS*, 275, 720
- Navarro, J. F., Frenk, C. S., & White, S. D. M. 1996, *The Astrophysical Journal*, 462, 563
- Navarro, J. F., Frenk, C. S., & White, S. D. M. 1997, *ApJ*, 490, 493
- Newton, I. 1804, *Opticks: or, A treatise of the reflections, refractions, inflexions and colours of light. Also two treatises of the species and magnitude of curvilinear figures (London : Printed for Sam Smith, and Benj. Walford, printers to the Royal Society, at the prince's Arms in St. Paul's Church-yard)*
- Niemiec, A., Jauzac, M., Eckert, D., et al. 2023, *Monthly Notices of the Royal Astronomical Society*, 524, 2883
- Niemiec, A., Jauzac, M., JullMultiscale cluster lens mass o, E., et al. 2020, *Monthly Notices of the Royal Astronomical Society*, 493, 3331
- Normann, B. D. & Clarkson, C. 2020, *General Relativity and Gravitation*, 52
- Okura, Y., Umetsu, K., & Futamase, T. 2007, *The Astrophysical Journal*, 660, 995–1002
- Okura, Y., Umetsu, K., & Futamase, T. 2008, *ApJ*, 680, 1
- Pizzuti, L., Saltas, I. D., Umetsu, K., & Sartoris, B. 2022, *Monthly Notices of the Royal Astronomical Society*, 512, 4280
- Ponente, P. P. & Diego, J. M. 2011, *Astronomy & Astrophysics*, 535, A119
- Rowe, B., Bacon, D., Massey, R., et al. 2013, *MNRAS*, 435, 822
- Saha, P. 2000, *AJ*, 120, 1654
- Saha, P., Williams, L. L., & AbdelSalam, H. 1999, arXiv preprint astro-ph/9909249
- Saha, P. & Williams, L. L. R. 2006, *ApJ*, 653, 936
- Schaathun, H. G., Normann, B. D., Austnes, E. L., et al. 2023a, in *Proceedings of the 30th European Conference on Modelling and Simulation*, ed. E. Vicario, R. Bandinelli, V. Fani, & M. Mastroianni (ECMS - European Council for Modelling and Simulation), Florence, Italy, 21–23 June 2023
- Schaathun, H. G., Normann, B. D., & Solevåg-Hoti, K. 2023b, Norsk IKT-konferanse for forskning og utdanning, to be presented at *Norsk Informatikkonferanse* in Stavanger 28–29 November 2023
- Schneider, P. 1995, *Astronomy & Astrophysics*, 302, 639
- Schneider, P., Ehlers, J., & Falco, E. 1999, *Gravitational lenses*, Vol. 33 (Springer Berlin Heidelberg), 560
- Schneider, P. & Er, X. 2008, *Astronomy & Astrophysics*, 485, 363
- Schneider, P., King, L., & Erben, T. 2000, *Astronomy and Astrophysics*, 353, 41
- Schneider, P., Kochanek, C., & Wambsganss, J. 2006, *Gravitational lensing: strong, weak and micro: Saas-Fee advanced course 33*, Vol. 33 (Springer Science & Business Media), 150–152
- Schneider, P. & Seitz, C. 1995, *A&A*, 294, 411
- Schneider, P. & Sluse, D. 2014, *Astronomy & Astrophysics*, 564, A103
- Seitz, C. & Schneider, P. 1995, *A&A*, 297, 287
- Seitz, C. & Schneider, P. 1997, *A&A*, 318, 687
- Seitz, S. & Schneider, P. 1996, *A&A*, 305, 383
- Seitz, S. & Schneider, P. 2001, *A&A*, 374, 740
- Seitz, S., Schneider, P., & Bartelmann, M. 1998, *A&A*, 337, 325
- Sendra, I., Diego, J. M., Broadhurst, T., & Lazkoz, R. 2014, *Monthly Notices of the Royal Astronomical Society*, 437, 2642
- Smith, G. P., Kneib, J.-P., Smail, I., et al. 2005, *Monthly Notices of the Royal Astronomical Society*, 359, 417
- Soucail, G., Mellier, Y., Fort, B., Hammer, F., & Mathez, G. 1987, *Astronomy and Astrophysics*, 184, L7
- Squires, G. & Kaiser, N. 1996, *The Astrophysical Journal*, 473, 65
- Tchernin, C., Bartelmann, M., Huber, K., et al. 2018, *Astronomy & Astrophysics*, 614, A38
- Tchernin, C., Majer, C. L., Meyer, S., et al. 2015, *Astronomy & Astrophysics*, 574, A122
- Torres-Ballesteros, D. A. & Castañeda, L. 2023, *Monthly Notices of the Royal Astronomical Society*, 518, 4494
- Troxel, M. A. & Ishak, M. 2015, *Phys. Rep.*, 558, 1
- Tyson, J. A., Valdes, F., & Wenk, R. A. 1990, *Astrophysical Journal*, 349, L1
- Umetsu, K. 2013, *The Astrophysical Journal*, 769, 13
- Umetsu, K. & Broadhurst, T. 2008, *The Astrophysical Journal*, 684, 177
- Umetsu, K., Broadhurst, T., Zitrin, A., Medezinski, E., & Hsu, L.-Y. 2011, *Astrophys. J.*, 729, 127
- Vines, J. 2015, *General Relativity and Gravitation*, 47
- Viola, M., Melchior, P., & Bartelmann, M. 2012, *MNRAS*, 419, 2215
- Webster, R. L. 1985, *MNRAS*, 213, 871
- Zwicky, F. 1937a, *Physical Review*, 51, 290
- Zwicky, F. 1937b, *Physical Review*, 51, 679

Appendix A: Study selection

Table A.1: The table presents the short-list of 29 papers selected for study through the structured search. The column ‘MSD’ categorizes how the mass-sheet degeneracy is treated in the study. ‘z’ means sources at different redshifts. ‘magn’ is short for magnification. ‘ \leq Flex’ means that both shear and flexion data has been used.

Authors	Title	Free-form?	ψ or κ ?	MSD	WL data	Method
AbdelSalam et al. (1998a)	Mass reconstruction of combined strong & weak lensing	Yes	κ	z	Shear	Inverse
AbdelSalam et al. (1998b)	Nonparametric reconstruction of Abell 2218 from combined weak and strong lensing	Yes	κ	z	Shear	Inverse
AbdelSalam et al. (1997)	Cluster mass profile from lensing	Yes	κ	z	Shear	Inverse
Birrer et al. (2017)	Line-of-sight effects in strong lensing: putting theory into practice	No	κ ?	Discussed	Shear	Inverse?
Bradač (2005)	Strong and weak lensing united: the cluster mass distribution of the most X-ray luminous cluster RX J1347-1145	Yes	ψ	z	Shear	Inverse
Bradač et al. (2005a)	Strong & weak lensing united: The cluster mass distribution of RX J1347-1145	Yes	ψ	z	Shear	Inverse
Bradač et al. (2005)	Strong and weak lensing united - I. The combined strong and weak lensing cluster mass reconstruction method	Yes	ψ	z	Shear	Inverse
Bradač et al. (2005)	Strong and weak lensing united - II. The cluster mass distribution of the most X-ray luminous cluster RX J1347.5-1145	Yes	ψ	z	Shear	Inverse
Bradač et al. (2005)	Strong and weak lensing united. III. Measuring the mass distribution of the merging galaxy cluster IES 0657-558	Yes	ψ	z	Shear	Inverse
Bradač et al. (2009)	Focusing cosmic telescopes: exploring redshift z 5-6 galaxies with the bullet cluster 1E0657-56	Yes	ψ	z	Shear	Inverse
Cacciato et al. (2006)	Combining weak and strong lensing in cluster potential reconstruction	Yes?	ψ	scale	Shear	Inverse
Cha et al. (2024)	Precision MARS Mass Reconstruction of A2744: Synergizing the Largest Strong-lensing and Densest Weak-lensing Data Sets from JWST	Yes	κ	scale	Shear	Inverse
Deb et al. (2012)	Mass reconstruction using Particle Based Lensing II: Quantifying substructure with strong + weak lensing and X-rays	Yes	ψ	z(+ scale?)	Shear	Inverse
Diego (2014)	An improved dark matter map from weak and strong lensing in A1689	Yes	κ	Discussed	Shear	Inverse
Diego et al. (2007)	Combined weak and strong lensing data with WSLAP	Yes	κ	Discussed	Shear	Inverse
Er et al. (2010)	Mass reconstruction by gravitational shear and flexion	Yes	ψ	z?	\leq Flex.	Inverse
Leonard et al. (2007)	Gravitational shear, flexion and strong lensing in Abell 1689	Partially	κ	Discussed	\leq Flex.	Direct
Liesenborgs et al. (2020)	Extended lens reconstructions with grale: exploiting time-domain, substructural and weak lensing information	Yes	κ	Discussed	Shear	Inverse
Merten et al. (2009)	Combining weak and strong cluster lensing: applications to simulations and MS 2137	Yes	ψ	Discussed	Shear	Inverse
Merten (2016)	Mesh-free free-form lensing - I. Methodology and application to mass reconstruction	Yes	ψ	Discussed	Shear	Inverse
Natarajan et al. (2009)	The survival of dark matter halos in the cluster Cl0024+ 16	No	κ	Not discussed	Shear	Inverse
Niemiec et al. (2020)	Hybrid-lensool: a self-consistent algorithm to model galaxy clusters with strong- and weak-lensing simultaneously	Partially	κ	not discussed	Shear	Inverse
Normann & Clarkson (2020)	Recursion relations for gravitational lensing	Yes	ψ	not discussed	n th order	Direct
Niemiec et al. (2023)	Beyond the ultra-deep frontier fields and legacy observations (BUFFALO): a high-resolution strong+weak lensing view of Abell 370	Partially	κ	Not discussed	Shear	Inverse
Ponente & Diego (2011)	Systemics in lensing reconstruction: dark matter rings in the sky?	Yes	κ	z	Shear	Inverse
Saha et al. (1999)	Cluster reconstruction from combined strong and weak lensing	Yes	κ	z	Shear	Inverse
Schneider & Seitz (1995)	Steps towards nonlinear cluster inversion through gravitational distortions.					
	I. Basic considerations and circular clusters	Yes	κ	Discussed	Shear	direct
Umetsu (2013)	Model-free multi-probe lensing reconstruction of cluster mass profiles	Yes	κ	z and magn	Shear	Inverse
Umetsu & Broadhurst (2008)	Combining lens distortion and depletion to map the mass distribution of A1689	Yes	κ	z and magn	Shear	Inverse